

Electronic and optical properties of magnesium and calcium hydroxides: The role of covalency and many-body effects

Smagul Zh. Karazhanov

Department for Solar Energy, Institute for Energy Technology, NO-2027 Kjeller, Norway

Aleksandr Pishtshev

Institute of Physics, University of Tartu, 510411 Tartu, Estonia

M. Klopov

Department of Physics, Tallinn University of Technology, 19086 Tallinn, Estonia

Abstract

Magnesium and calcium hydroxides $X(\text{OH})_2$ ($X=\text{Mg}, \text{Ca}$) are the multifunctional materials that have many important applications in industry, technology and research. In solid state electronics, the emerging applications of these compounds are related to photovoltaic devices. In the present paper we review electronic properties of $X(\text{OH})_2$, band gaps, work function, features of chemical bonding, and discuss theoretically predicted exciton effects.

Keywords: magnesium hydroxide, brucite, calcium hydroxide, lime, crystal structure, electronic structure, chemical bonding, optical properties, exciton

Email addresses: smagulk@ife.no (Smagul Zh. Karazhanov),
aleksandr.pishtshev@ut.ee (Aleksandr Pishtshev), mihhail.klopov@ttu.ee (M. Klopov)

Preprint submitted to Name of the journal

February 26, 2015

1. Introduction

Recent advances in chemical technology combined with modern quantum mechanical methods allow one to predict and construct materials possessing many desired properties such as electronic, mechanical, optical, thermal, or others, which are principally important for different technological applications. However, the design of a novel multifunctional material requires numerous efforts, and the corresponding production costs are often connected with high investment risks. On the other hand, compounds which have abundance in nature might be considered as attractive from technological and economical points of view. Functionality of the compounds can be extended by doping with different types of impurities [1, 2]. The compounds (or most of them) can be related to the class of multifunctional materials because they are typically endowed with different sets of properties depending mainly on the naturally occurring composition of elements and the specific features of chemical bonding. In the present paper, the focus is made on the case of relatively simple alkaline-earth hydroxides $X(\text{OH})_2$ ($X=\text{Mg}$ and Ca), which are interesting in the context of multifunctionality because they exhibit a variety of useful properties. It is worthy of note that the elements composing $X(\text{OH})_2$ are widely available, low cost and non-toxic; magnesium is the eighth and calcium is the fifth most abundant elements in the earths crust. Their price is much lower than the price of indium and tin, and close to that of zinc. It is also well known that hydrogen, and oxygen are the most abundant elements in the universe.

The multifunctional hydroxides $X(\text{OH})_2$ have found a wide range of applications in medicine, environment, and electronic technology. Studies of these materials have already been the topic for extensive scientific research. Portlandite $\text{Ca}(\text{OH})_2$ is one of the most important inorganic materials in lime industries. In addition to the significant usage in building and engineering fields its functional properties are widely implemented in a variety of applications; the primers range from water treatment methods [3] to dental therapy [4]. Brucite $\text{Mg}(\text{OH})_2$ has also demonstrated similar effectiveness in waste water treatments [5–8] and a high antibacterial efficiency against several tested bacterial strains [9]. There is an interesting experience of employing $\text{Mg}(\text{OH})_2$ as a precursor for magnesium oxide refractory ceramics [10], or as a flame retardant in various polymer compositions and smoke suppressants [10–12].

37 **2. Applications in solar cells**

38 $X(\text{OH})_2$ is the emerging material for solar cell applications. It has been
39 employed for a surface modification of TiO_2 nanoparticles, which is one of
40 the promising strategies in improving energy conversion efficiency. For ex-
41 amples, coating the TiO_2 nanoparticles with a metal oxide has enhanced the
42 conversion efficiency of the cell. It was reported [13, 14] that a coating of
43 TiO_2 by $\text{Mg}(\text{OH})_2$ has improved open circuit voltage of dye-sensitized solar
44 cell. Suppression of charge carrier recombination at the interface of the dye-
45 sensitized solar cells has been reported [15] for $\text{Ca}(\text{OH})_2$. $\text{Mg}(\text{OH})_2$ has been
46 used as a buffer layer in CuInSe [16, 17] cells and as a passivation layer in
47 dye-sensitized [13–15, 18] composite solar cells.

48 As discussed below, excitons possessing large binding energy might exist
49 in $X(\text{OH})_2$ at room temperature. Once free electrons and holes are created
50 in the material, they might be bound into excitons. Consequently, concentra-
51 tion of free electrons and holes in $X(\text{OH})_2$ might be much smaller than that
52 of excitons. Although the excitons are neutral, they can indirectly influence
53 on charge carrier concentration by dissociation and annihilation as well as
54 by modulating the charge state of impurities, which will also influence on
55 electrical current transport. There is no work estimating relation of concen-
56 tration of excitons to that of free charge carriers and diffusion coefficient of
57 excitons.

58 Recently, an exciting property of carbon doped $\text{Mg}(\text{OH})_2$ films was re-
59 ported in Refs. [1, 19]. It was demonstrated that such modified material is
60 not only transparent in visible range of sunlight, but it is also electrically well
61 conducting with conductivity of ~ 167 S/cm. Note that $\text{Mg}(\text{OH})_2$ itself is a
62 wide band gap insulator. However, upon doping by C impurity, $\text{Mg}(\text{OH})_2$,
63 in addition to being transparent to sunlight, becomes electrically well con-
64 ducting. This finding is expected to broaden the applications of $\text{Mg}(\text{OH})_2$ in
65 photovoltaic devices, smart windows, and other semiconductor devices.

66 **3. Properties**

67 *3.1. Structural properties*

68 Structural, morphological, and vibrational properties of $X(\text{OH})_2$ are the
69 most systematically studied ones (see, e.g., Refs. [20–28]). Both magnesium
70 and calcium hydroxides possess trigonal structure of space group $P\bar{3}m1$, no.
71 164, with one formula unit per the unit cell [29–32]. No other polymorphs of
72 $\text{Mg}(\text{OH})_2$ and $\text{Ca}(\text{OH})_2$ have been reported in literature [33, 34].

73 *3.2. Band parameters*

74 Implementation of $X(\text{OH})_2$ in solar cells and other semiconductor devices
75 requires an understanding of its fundamental physical and chemical proper-
76 ties. One of the important materials parameters to know is the band gap E_g .
77 There is no systematic study of this parameter for $X(\text{OH})_2$ performed for
78 more or less pure compound at low temperatures. The existing experimental
79 data have been obtained for $\text{Mg}(\text{OH})_2$ synthesized by chemical method and
80 the measurements have been performed at room temperature. The obtained
81 band gaps have a large scatter: 5.17 eV for the thin film samples [16], 5.70 eV
82 for $\text{Mg}(\text{OH})_2$ nanodisks [35] and about 7.6 eV [36] for the bulk. Theoret-
83 ically estimated band gaps are predicted to be in the range of 7.7-8.3 eV for
84 $\text{Mg}(\text{OH})_2$ and 7.3-7.6 eV for $\text{Ca}(\text{OH})_2$ [37].

85 Knowledge of effective masses is also important for characterization of
86 charge carrier transport through the $X(\text{OH})_2$ layer. There are no experi-
87 mental data related to their measurements. Based on the electronic structure
88 studies theoretical calculations have been performed [37]. Analysis showed
89 that the conduction band effective masses are about 0.13 m_0 for $\text{Mg}(\text{OH})_2$
90 (in the unit of the free-electron mass (m_0)) and 0.18 m_0 for $\text{Ca}(\text{OH})_2$. These
91 masses are close to the 0.24 m_0 for ZnO [38]. The hole masses at the valence
92 band maximum are 3.06 m_0 for $\text{Mg}(\text{OH})_2$ and 0.44 m_0 for $\text{Ca}(\text{OH})_2$, which
93 are quite different than the mass 2.74 m_0 for ZnO.

94 Work function of electrons (WF) for $X(\text{OH})_2$ is one of the important
95 parameters, which is very sensitive to surface properties such as thermionic
96 emission, photoemission, catalysis, etc. [39]. There are no experimental
97 investigations of WF for the $X(\text{OH})_2$ materials. Theoretical estimates based
98 on *ab initio* studies [37] show 4.46 eV for $\text{Mg}(\text{OH})_2$ and 4.78 eV for $\text{Ca}(\text{OH})_2$,
99 respectively.

100 *3.3. Chemical bonding: the role of covalency*

101 The most interesting aspect of chemical design in $\text{Mg}(\text{OH})_2$ and $\text{Ca}(\text{OH})_2$
102 hydroxides is that a rich behavior of these materials are based mainly on
103 two principal factors; both of them are associated with the hydroxyl an-
104 ions $(\text{OH})^-$. The first factor of structure-specific nature is connected with a
105 layered complexity of the bulk along c axes: it is determined by the hexag-
106 onal close packing of the hydroxide anions in the crystal lattice [34]. The
107 second factor is that the three-body structural $X\text{--O--H}$ block consisting of
108 the almost fully oxidized metal cation and $(\text{OH})^-$ anion is responsible for a
109 common chemical stability in terms of a spatial localization of the electronic

110 charge [37]. That is, the oxygen playing the role of a principal oxidizer forms
111 the bridging site that balances electron-poor and electron-rich areas in such
112 a way to maintain a structural stability via consistent matching ionic and
113 covalent chemical interactions. At the macroscopic level, in terms of crystal
114 sublattices this implies that by incorporating a directional covalent bonding
115 into a host framing the hydroxyl anion redistributes the valence electron den-
116 sity to give rise to a sufficient rigidity of Mg^{2+} and Ca^{2+} cationic orderings,
117 which become electrostatically connected with the anionic sublattice of the
118 hydroxyl ions.

119 As follows from electron counting considerations the distribution of va-
120 lence electrons (formal charges) in the $X\text{--O--H}$ block gives the charges con-
121 sistent with the Lewis structure in which the octet rule is fulfilled. This
122 corresponds to the standard arrangements of the electronic pairs of the O^{2-}
123 ion in OH^- : one bond pair and three lone pairs.

124 Analysis of electron partitioning schemes (Fig. 1) in terms of electron
125 localization function (ELF) shows [37] that the electron-rich areas belong
126 mainly to the anionic subsystem of $X(\text{OH})_2$ where two regions of strong lo-
127 calization of valence electrons can be revealed. The first one is a vertically
128 oriented distribution of shared electron pairs which is associated with $s\text{-}p_z$
129 hybridization that governs covalent H--O bonding along c axis. The other is
130 arranged in ab -plane and corresponds to a manifold of non-bonding lone-pairs
131 associated with the occupied $2p_x, 2p_y$ oxygen orbitals. The theoretical cal-
132 culations indicate [37] that electronic states formed by these pairs contribute
133 into the top of the valence band, while the occupied $2p_z$ oxygen electronic
134 states (related to the covalent H--O bond) are significantly repelled toward
135 lower energies. Such nonplanar separation of the overall electron density with
136 respect to bonding and nonbonding regions, when states of $s - p_z$ hybridized
137 electrons lie lower than those corresponding to highest occupied $2p_x, 2p_y$ -
138 type orbitals of oxygen, will lead to a strong anisotropy of the electronic
139 and optical properties. Moreover, calculations of electronic partitions within
140 the unit cell space have shown that about 78% and 67% of the cell volume
141 in $\text{Mg}(\text{OH})_2$ and $\text{Ca}(\text{OH})_2$, respectively, is allocated to the arrangement of
142 valence electron pairs supplied by the oxygen of $(\text{OH})^-$ anion. This allows
143 us to predict the dominant role of the oxygen valence orbitals in electronic
144 responses of these materials.

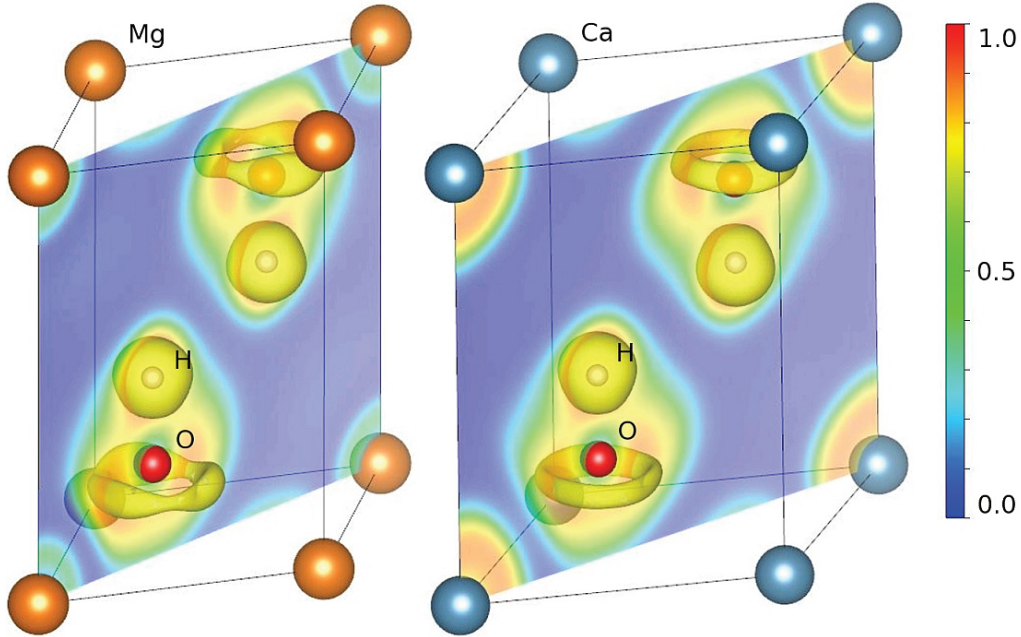


Figure 1: Representation of the valence ELF for $\text{Mg}(\text{OH})_2$ (left) and $\text{Ca}(\text{OH})_2$ (right) in (110) cut plane involving additional ELF isosurfaces for the hydroxyl anion evaluated at $\text{ELF} = 0.87$. The character of the regularity of the torus-shaped topology is determined by the minimization of electron-pair repulsion; this makes spatial arrangement of all three lone-pairs (the nonbonded domains) around the negative oxygen ion symmetrically localized in the $a - b$ plane. (Graphic illustration of this figure was made using the VESTA program[40]).

145 3.4. Excitons

146 It is well-established in a description of electronic responses common to
 147 ion-covalent materials that the contribution of many-body effects is directly
 148 determined by the degree of electronic charge localization [41, 42]. In this
 149 context, the multifunctional $X(\text{OH})_2$ are unique materials where the many-
 150 body effects should play crucial role in their optical properties. These prop-
 151 erties definitely have important implication for different applications of the
 152 materials in optoelectronic devices [16–18]. Importance of the many-body ef-
 153 fects in $X(\text{OH})_2$ becomes evident upon studies of the macroscopic dielectric
 154 constant ϵ_∞ , which serves as one of the important parameters characterizing
 155 how strong is the Coulomb interaction between an electron and a hole as well
 156 as how large is the exciton binding energy E_b . As it is well known, $\epsilon_\infty = 11.7$

157 Ref. [43] for Si with $E_b = 14.7$ meV Ref. [44], $\epsilon_\infty = 7.9$ Ref. [45] for ZnO with
 158 $E_b = 59$ meV Ref. [46], which means that excitons can exist at low tempera-
 159 tures in Si and at the room temperature in ZnO. Our theoretical studies [47]
 160 have shown that $\epsilon_\infty = 2.35$ for $\text{Mg}(\text{OH})_2$ and $\epsilon_\infty = 2.33$ for $\text{Ca}(\text{OH})_2$. Con-
 161 sequently, exciton binding energy in $X(\text{OH})_2$ is expected to be larger than
 162 that in ZnO. Theoretical studies of Ref. [47] by using the *ab initio* calcula-
 163 tions with the HSE06 hybrid functional [48–50] and GW approximation [51]
 164 combined with numerical solution of the Bethe-Salpeter equation [42, 52–55]
 165 (GW-BSE) predicted the possibility of existence of diverse number of exci-
 166 tonic states in the $X(\text{OH})_2$ hydroxides. The excitons possessing large binding
 167 energy of 0.46 eV for $\text{Mg}(\text{OH})_2$ and 0.85 eV $\text{Ca}(\text{OH})_2$ have been reported.
 168 They have been identified to be related to a strong localization of the hole
 169 and electron to oxygen $2p_x, 2p_y$ occupied states as well as to oxygen and
 170 metal s empty states, respectively. The corresponding model of the strongly
 171 localized excitons is schematically presented in Fig. 2.

172 A spectral peak near band edge corresponding to strongly localized ex-
 173 citons have been observed experimentally [16] in transmittance spectra of
 174 $\text{Mg}(\text{OH})_2$, samples of which were prepared by chemical bath deposition method.
 175 This peak corresponds to exciton binding energy of 0.53 eV, which is slightly
 176 larger than the theoretically predicted value. The discrepancy between the-
 177 ory and experiment of about 13 % is evidently connected with the fact that
 178 the measurements have been performed at room temperature, while the cal-
 culated GW-BSE results were obtained for $T = 0$ K.

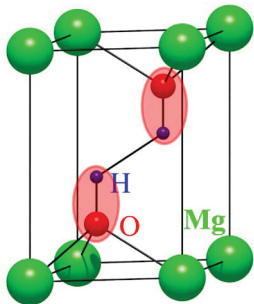


Figure 2: (Color online) Schematic presentation of excitons possessing large binding energy and located in the covalent sublattice of $\text{Mg}(\text{OH})_2$.

179

180 **4. Conclusion**

181 We have provided a short review of applications of multifunctional $X(\text{OH})_2$
182 ($X=\text{Mg}, \text{Ca}$) in photovoltaic devices as well as latest studies of electronic
183 structure of these materials. The materials possess unique optoelectronic
184 properties, can be synthesized by industrially viable methods, and consists
185 of abundant and non-toxic elements. Based on an analysis of the literature
186 and results of our research work we think that the $\text{Mg}(\text{OH})_2$ have good po-
187 tential for the use in fabricating optoelectronic and semiconductor devices.

188 **Acknowledgments**

189 The work was supported by the European Union through the European
190 Regional Development Fund (Centre of Excellence "Mesosystems: Theory
191 and Applications", TK114) and by the Estonian Science Foundation (grant
192 No 7296). Also this work has received financial and supercomputing support
193 from the Research Council of Norway within the FME project (192839) and
194 ISP NANOMAT project (181884).

195 **References**

- 196 [1] T. Kuji, M. Chiba, T. Honjo, K. Kotoda, Patent TW200923974. Trans-
197 parent conductive film and method for making same (2009).
- 198 [2] H. Shi, L. Chang, R. Jia, R. I. Eglitis, Ab initio calculations of hydroxyl
199 impurities in CaF_2 , J. Phys. Chem. C 116 (10) (2012) 6392–6400.
- 200 [3] T. Krüger, Sequestering carbon dioxide from the atmosphere by
201 enhancing the capacity of the oceans to act as a carbon sink,
202 <http://www.cquestrate.com/> (2008).
- 203 [4] C. Estrela, F. C. Pimenta, I. Y. Ito, L. L. Bammann, In vitro deter-
204 mination of direct antimicrobial effect of calcium hydroxide, J. Endod.
205 24 (1) (1998) 15–17.
- 206 [5] Q. Cao, F. Huang, Z. Zhuang, Z. Lin, A study of the potential ap-
207 plication of nano- $\text{Mg}(\text{OH})_2$ in adsorbing low concentrations of uranyl
208 tricarbonate from water, Nanoscale 4 (2012) 2423–2430.

- 209 [6] A. Gibson, M. Maniocha, White paper: The use of magnesium hydroxide
210 slurry for biological treatment of municipal and industrial wastewater,
211 Martin Marietta Magnesia Specialties, LLC (2004) 1–7.
- 212 [7] E. Ghali, W. Dietzel, K.-U. Kainer, General and localized corrosion of
213 magnesium alloys: A critical review, *J. Mater. Eng. Perform.* 13 (1)
214 (2004) 7–23.
- 215 [8] A. C. Snider, Hydration of magnesium oxide in the waste isolation pilot
216 plant, *Mat. Res. Soc. Symp. Proc.* 757 (2003) II8.3.1–6.
- 217 [9] H. Dhaouadi, H. Chaabane, T. Fathi, $\text{Mg}(\text{OH})_2$ nanorods synthesized
218 by a facile hydrothermal method in the presence of ctab, *Nano-Micro*
219 *Lett.* 3 (2011) 153–159.
- 220 [10] C. Henrist, J.-P. Mathieu, C. Vogels, A. Rulmont, R. Cloots, Morpholog-
221 ical study of magnesium hydroxide nanoparticles precipitated in dilute
222 aqueous solution, *J. Cryst. Growth* 249 (1–2) (2003) 321 – 330.
- 223 [11] J. Jančář, J. Kučera, Yield behavior of polypropylene filled with CaCO_3
224 and $\text{Mg}(\text{OH})_2$. I: "zero" interfacial adhesion, *Polym. Eng. Sci.* 30 (1990)
225 707–713.
- 226 [12] L. Shi, D. Li, J. Wang, S. Li, D. G. Evans, X. Duan, Synthesis, flame-
227 retardant and smoke-suppressant properties of a borate-intercalated lay-
228 ered double hydroxide, *Clays Clay Miner.* 53 (3) (2005) 294–300.
- 229 [13] T. A. N. Peiris, S. Senthilarasu, K. G. U. Wijayantha, Enhanced
230 performance of flexible dye-sensitized solar cells: Electrodeposition of
231 $\text{Mg}(\text{OH})_2$ on a nanocrystalline TiO_2 electrode, *J. Phys. Chem. C* 116 (1)
232 (2012) 1211–1218.
- 233 [14] T. A. Nirmal Peiris, K. G. U. Wijayantha, J. Garcia-Canadas, In-
234 sights into mechanical compression and the enhancement in performance
235 by $\text{Mg}(\text{OH})_2$ coating in flexible dye sensitized solar cells, *Phys. Chem.*
236 *Chem. Phys.* 16 (2014) 2912–2919.
- 237 [15] Promotion of charge transport in low-temperature fabricated TiO_2 elec-
238 trodes by curing-induced compression stress, *Electroch. Acta* 100 (0)
239 (2013) 85–92.

- 240 [16] C.-H. Huang, Y.-L. Jan, W.-C. Lee, Investigation of Mg(OOH) films
241 prepared by chemical bath deposition as buffer layers for Cu(InGa)Se₂
242 solar cells, *J. Electrochem. Soc.* 158 (9) (2011) H879–H888.
- 243 [17] H. Miyazaki, R. Mikami, A. Yamada, M. Konagai, Chemical-bath-
244 deposited ZnO and Mg(OH)₂ buffer layer for Cu(InGa)Se₂ solar cells,
245 *Jpn. J. Appl. Phys., Part 1* 45 (4A) (2006) 2618–2620.
- 246 [18] J.-H. Yum, S. Nakade, D.-Y. Kim, S. Yanagida, Improved performance
247 in dye-sensitized solar cells employing TiO₂ photoelectrodes coated with
248 metal hydroxides, *J. Phys. Chem. B* 110 (7) (2006) 3215–3219.
- 249 [19] M. Chiba, D. Endo, K. Haruta, H. Kimura, H. Kiyota, Semiconduc-
250 tive properties of alternating mg/c multi-layer films with hydroxylation
251 treatment, in: *Symposium F Oxide Semiconductors and Thin Films*,
252 Vol. 1494 of *MRS Proceedings*, 2013, pp. 197–202.
- 253 [20] D. E. Haycock, M. Kasrai, C. J. Nicholls, D. S. Urch, The electronic
254 structure of magnesium hydroxide (brucite) using x-ray emission, x-ray
255 photoelectron, and auger spectroscopy, *J. Chem. Soc., Dalton Trans.*
256 (1978) 1791–1796.
- 257 [21] Y. Zhu, G. Wu, Y.-H. Zhang, Q. Zhao, Growth and characterization of
258 Mg(OH)₂ film on magnesium alloy az31, *Appl. Surf. Sci.* 257 (14) (2011)
259 6129 – 6137.
- 260 [22] K. Azuma, T. Oda, S. Tanaka, Vibration analysis of O–H stretching
261 mode in Mg(OH)₂, Ca(OH)₂, LiOH, and NaOH by plane-wave pseu-
262 dopotential DFT calculation, *Comput. Theor. Chem.* 963 (1) (2011)
263 215–220.
- 264 [23] P. Baranek, A. Lichanot, R. Orlando, R. Dovesi, Structural and vibra-
265 tional properties of solid Mg(OH)₂ and Ca(OH)₂ performances of various
266 hamiltonians, *Chem. Phys. Lett.* 340 (3-4) (2001) 362–369.
- 267 [24] B. Weckler, H. D. Lutz, Near-infrared spectra of M(OH)Cl (M = Ca, Cd,
268 Sr), Zn(OH)F, Cd(OH)₂, Sr(OH)₂, and brucite-type hydroxides M(OH)₂
269 (M = Mg, Ca, Mn, Fe, Co, Ni, Cd), *Spectrochim. Acta, Part A* 52 (11)
270 (1996) 1507–1513.

- 271 [25] H. D. Lutz, H. Müller, M. Schmidt, Lattice vibration spectra. part lxxxii.
272 brucite-type hydroxides $M(\text{OH})_2$ ($M = \text{Ca}, \text{Mn}, \text{Co}, \text{Fe}, \text{Cd}$) - IR and
273 Raman spectra, neutron diffraction of $\text{Fe}(\text{OH})_2$, *J. Mol. Struct.* 328 (0)
274 (1994) 121–132.
- 275 [26] J. C. Owrutsky, N. H. Rosenbaum, L. M. Tack, R. J. Saykally, The
276 vibration-rotation spectrum of the hydroxide anion (OH^-), *J. Chem.*
277 *Phys.* 83 (10) (1985) 5338–5339.
- 278 [27] R. L. Frost, J. T. Kloprogge, Infrared emission spectroscopic study of
279 brucite, *Spectrochim. Acta, Part A* 55 (11) (1999) 2195–2205.
- 280 [28] S. Rauegi, P. L. Silvestrelli, M. Parrinello, Pressure-induced frustration
281 and disorder in $\text{Mg}(\text{OH})_2$ and $\text{Ca}(\text{OH})_2$, *Phys. Rev. Lett.* 83 (1999)
282 2222–2225.
- 283 [29] L. Desgranges, G. Calvarin, G. Chevrier, Interlayer interactions in
284 $\text{Mg}(\text{OH})_2$: a neutron diffraction study of $\text{Mg}(\text{OH})_2$, *Acta Crystallogr.,*
285 *Sect. B: Struct. Sci.* 52 (1) (1996) 82–86.
- 286 [30] M. Catti, G. Ferraris, S. Hull, A. Pavese, Static compression and H
287 disorder in brucite, $\text{Mg}(\text{OH})_2$, to 11 GPa: a powder neutron diffraction
288 study, *Phys. Chem. Miner.* 22 (3) (1995) 200–206.
- 289 [31] L. Desgranges, D. Grebille, G. Calvarin, G. Chevrier, N. Floquet, J. C.
290 Niepce, Hydrogen thermal motion in calcium hydroxide: $\text{Ca}(\text{OH})_2$, *Acta*
291 *Crystallogr., Sect. B: Struct. Sci.* 49 (5) (1993) 812–817.
- 292 [32] W. R. Busing, H. A. Levy, Neutron diffraction study of calcium hydrox-
293 ide, *J. Chem. Phys.* 26 (3) (1957) 563–568.
- 294 [33] H. Oswald, R. Asper, Bivalent metal hydroxides, in: R. M. A. Lieth
295 (Ed.), *Preparation and Crystal Growth of Materials with Layered Struc-*
296 *tures, Vol. I of Physics and Chemistry of Materials with Layered Struc-*
297 *tures*, Springer, 1977, pp. 71–140.
- 298 [34] F. Freund, Highly ionic hydroxides: unexpected proton conductivity in
299 $\text{Mg}(\text{OH})_2$ and homologues, in: P. Colomban (Ed.), *Proton conductors.*
300 *Solids, membranes and gels - materials and devices, Vol. 2 of Chem. Solid*
301 *State Mater.*, Cambridge University Press, 1992, Ch. 9, pp. 138–157.

- 302 [35] L. Kumari, W. Z. Li, C. H. Vannoy, R. M. Leblanc, D. Z. Wang,
303 Synthesis, characterization and optical properties of $\text{Mg}(\text{OH})_2$ micro-
304 /nanostructure and its conversion to MgO , *Ceramics International* 35 (8)
305 (2009) 3355–3364.
- 306 [36] T. Murakami, T. Honjo, T. Kuji, Dos calculation analysis of new trans-
307 parent conductor $\text{Mg}(\text{OH})_2\text{-C}$, *Mater. Trans.* 52 (8) (2011) 1689–1692.
- 308 [37] Pishtshev, A., Karazhanov, S. Zh., Klopov, M., Materials properties
309 of magnesium and calcium hydroxides from first-principles calculations,
310 *Comput. Mater. Sci* (2014) in Press.
- 311 [38] K. Hümmer, Interband magnetoreflexion of ZnO , *Phys. Status Solidi B*
312 56 (1) (1973) 249–260.
- 313 [39] A. Subrahmanyam, S. Kumar, *The Kelvin Probe for Surface Engineer-*
314 *ing: Fundamentals and Design*, CRC Press, New Delhi, Chennai, Mum-
315 bai, Bengaluru, Kolkata, Thiruvananthapuram, Lucknow, 2010.
- 316 [40] K. Momma, F. Izumi, *VESTA3* for three-dimensional visualization of
317 crystal, volumetric and morphology data, *J. Appl. Crystallogr.* 44 (6)
318 (2011) 1272–1276.
- 319 [41] Meskini, N., Hanke, W., Mattausch, H.J., Balkanski, M., Zouaghi, M.,
320 The absorption spectrum of a heteropolar crystal : the role of many-
321 particle effects, *J. Phys. France* 45 (10) (1984) 1707–1715.
- 322 [42] M. Dvorak, S.-H. Wei, Z. Wu, Origin of the variation of exciton binding
323 energy in semiconductors, *Phys. Rev. Lett.* 110 (2013) 016402.
- 324 [43] Dunlap, W. C., Watters, R. L., Direct measurement of the dielectric
325 constants of silicon and germanium, *Phys. Rev.* 92 (1953) 1396–1397.
- 326 [44] K. L. Shaklee, R. E. Nahory, Valley-orbit splitting of free excitons: The
327 absorption edge of si, *Phys. Rev. Lett.* 24 (1970) 942–945.
- 328 [45] H. Yoshikawa, S. Adachi, Optical constants of zno , *Jpn. J. Appl. Phys.*
329 36 (10) (1997) 6237.
- 330 [46] P. Y. Yu, M. Cardona, *Fundamentals of Semiconductors*, Springer, New
331 York, 2005.

- 332 [47] Pishtshev, A., Karazhanov, S. Zh., Klopov, M., Excitons in $\text{Mg}(\text{OH})_2$
333 and $\text{Ca}(\text{OH})_2$ from *ab initio* calculations, Solid State Commun. 193 (0)
334 (2014) 11–15.
- 335 [48] J. Heyd, G. E. Scuseria, M. Ernzerhof, Hybrid functionals based on a
336 screened coulomb potential, J. Chem. Phys. 118 (18) (2003) 8207–8215.
- 337 [49] A. V. Krukau, O. A. Vydrov, A. F. Izmaylov, G. E. Scuseria, Influence
338 of the exchange screening parameter on the performance of screened
339 hybrid functionals, J. Chem. Phys. 125 (22) (2006) 224106.
- 340 [50] T. M. Henderson, J. Paier, G. E. Scuseria, Accurate treatment of solids
341 with the HSE screened hybrid, Phys. Status Solidi B 248 (4) (2011)
342 767–774.
- 343 [51] L. Hedin, New method for calculating the one-particle Green’s function
344 with application to the electron-gas problem, Phys. Rev. 139 (1965)
345 A796–A823.
- 346 [52] M. Rohlfing, S. G. Louie, Electron-hole excitations in semiconductors
347 and insulators, Phys. Rev. Lett. 81 (1998) 2312–2315.
- 348 [53] L. X. Benedict, E. L. Shirley, R. B. Bohn, Optical absorption of insula-
349 tors and the electron-hole interaction: An *Ab Initio* calculation, Phys.
350 Rev. Lett. 80 (1998) 4514–4517.
- 351 [54] S. Albrecht, L. Reining, R. Del Sole, G. Onida, *Ab Initio* calculation
352 of excitonic effects in the optical spectra of semiconductors, Phys. Rev.
353 Lett. 80 (1998) 4510–4513.
- 354 [55] D. Y. Qiu, F. H. da Jornada, S. G. Louie, Optical spectrum of MoS_2 :
355 Many-body effects and diversity of exciton states, Phys. Rev. Lett. 111
356 (2013) 216805.